Supplementary Tables to Tralau *et al.*

Supplementary table 1. Plasmids used to express different versions of DMGO.

Plasmid	Gene(s)	Resistance, replicon	Reference
pDMGO	dmg, *wt*	Amp, ColE1	(1)
pEH1	dmg-operon, *wt*	Amp, ColE1	(2)
pDMGO^{D552A}	*dmg*, expressing A instead of D at aa position 552	Amp, ColE1	this study
pDMGO^{D552N}	*dmg*, expressing N instead of D at aa position 552	Amp, ColE1	this study
pDMGO$^{\Delta Cterm}$	*dmg*, expressing aa 1-435	Amp, ColE1	this study
pDMGO^{Y259F}	*dmg*, expressing F instead of Y at aa position 259	Amp, ColE1	(2)
pColaGfp dmg^{Y259F}	*gfp-frm* promotor fusion and *dmg* expressing F instead of Y at aa position 259	Km, pColA	this study

1. Leys D, Basran J, Scrutton NS. (2003) Channelling and formation of 'active' formaldehyde in dimethylglycine oxidase. *EMBO J* 22:4038-4048

2. Meskys R, Harris RJ, Casaite V, Basran J, Scrutton NS (2001) Organization of the genes involved in dimethylglycine and sarcosine degradation in *Arthrobacter* spp.. Implications for glycine betaine catabolism. *Eur J Biochem* 268:3390-3398

Supplementary table 2. Primers used for cloning.

Primer*	Sequence†	T_a‡	Target
gfpuv*Xce*I_f	5' - ggtagaaaacATGTCTAAAGGAGA - 3'	52 °C	*gfp*, fusion to the *frmR*-promotor
gfpuv*Pag*I_f	5' - ggtagaaatcATGAGTAAAGGAGA - 3'	52 °C	*gfp*, fusion to *frmA* Shine Dalgarno-sequence
gfpuv*Hind*III_r	5' - tcagttggaaaagcTTATTTGTAGAG - 3'	52 °C	*gfp*
frm_f-635	5' - ggtctttgcccgccaggat - 3'	59 °C	*frm*-operon, template for subsequent PCR
frmA_r527	5' - cggccccttcgtgaccgagaa - 3'	59 °C	*frm*-operon, template for subsequent PCR
frm_f-367 *EcoR*Ilong	5' - agccgcggaattcgtgcttacacctatgac - 3'	66 °C	*frmR*-promotor region
frm_r-2*XceI*	5' - CTTCCGGAGTACTGGGCATGTCGCAC CTCATCATCTGCATgg - 3'	66 °C	*frmR*-promotor region
frm_f-367*EcoR*I	5' - agccgcggaattcgtgcttacac - 3'	60 °C	*frmR*-promotor region
frmA_r339*Pag*I	5' - GATTTCATgactcgctcttcctcaatatgg - 3'	60 °C	ATG of *frmA*
dmg_f*Nde*I	5' - gacatgattacgaacatATGGCATCGAC - 3'	55-50 °C, touchdown	*dmg*, for cloning into MCS2 of pColaDuet-1
dmg_r*Fse*I	5' - gcgtgtcccggccggccct- 3'	55-50 °C, touchdown	*dmg*, for cloning into MCS2 of pColaDuet-1

* f(orward) and r(everse) denote the orientation of the primers, subsequent numbers indicate the position of the primer in regard to the corresponding ATG.

† Coding sequences are capitalized and restriction sites for the enzymes indicated in the primer name are underlined.

‡ Annealing temperature used for the corresponding primer. PCR was done in a total volume 50 µl, using ABgene Extensor polymerase mixture (Abgene, UK) together with the supplied buffer 1 and purified plasmid DNA (500 pg/µl, for *gfp*), genomic DNA (500 pg/µl, for the *frm*-operon template), purified PCR product (0.7 pg/µl, for mutated *frm*-inserts) or ligated PCR product (50 pg/µl, for the *frm-gfp* fusions) as template. Fusions of *gfp* to the corresponding region of the *frm*-operon were done using the inserted *Xce*I or the *Pag*I sites respectively and the ligated construct was reamplified prior to insertion into pET24(+) using *EcoR*I and *Hind*III.

Supplementary table 3. DMGO^{D552A} data collection and refinement statistics.

Space Group	C222
Unit Cell (Å)	a=71.2 b=224.6 c=119.4
Resolution (Å)	20-2.0 (2.1-2.0)
Total Reflections	168,852
Unique Reflections	65,012
Completeness (%)	97.1 (93.4)
Redundancy	4.8 (3.2)
R_{merge}	7.0 (37.5)
I/sigI	11.8 (2.1)
R_{work}	15.3 (17.3)
R_{free}	20.0 (22.7)
rmsd angle (°)	1.570
rmsd bond length (Å)	0.016
Ramachandran outliers	0% (0/825)
Ramachandran favored	98.2 5 (810/825)

Supplementary Figures to Tralau *et al.*

Supp. Fig. 1. Overview of the *in vivo* formaldehyde reporter system
Schematic overview of cellular reactions studied within an *E. coli* formaldehyde detoxification deficient strain with DMGO represented as blue box. Key molecular species respectively detected *in vivo* and *in vitro* are formaldehyde (in red) and hydrogen peroxide (in blue).

Supp. Fig. 2. Molecular dynamics trajectories of lactone intermediate in DMGO.
(A) A single molecular dynamics trajectory of the unprotonated lactone intermediate diffusion in DMGO cavity revealing an abrupt and rapid transfer event between active sites between 3 and 4 ns. I, II, III, and IV indicate the initial positions used to run shorter simulations shown in panel B.
(B) Several shorter trajectories starting from individual positions obtained in the panel A trajectory, the original trajectory is drawn as bold line, the individual shorter simulation trajectories are represented as thin lines. These reveal the individual paths to be irreproducible and the transfer between active sites to be a highly stochastic event indicating unguided diffusion occurs. Similar conclusions were reached for the other iminium forms (see Suppl. Figs. 6-7)

Supp. Fig. 3. Brownian dynamics simulations of hydrated formaldehyde diffusion in DMGO cavity.
The volume explored by formaldehyde during 20 000 BD simulations was calculated as described in Materials and Methods, and is rendered as blue mesh. FAD and folinic acid molecules are respectively represented in cyan and green Van der Waals spheres. Alternative exit channel is indicated by an arrow.

Supp. Fig. 4. DMGO does not protect against high levels of intracellular formaldehyde. Cells containing the reporter system ± Y259F DMGO were grown as batch cultures in the presence of different concentrations of N-methyltryptophan. The uncalibrated fluorescence as measured using the microtitre plate assay reveals both clones to yield similar levels of intracellular formaldehyde. This indicates that DMGO does not contribute to the detoxification of intracellular formaldehyde.

Supp. Fig. 5. Molecular dynamics trajectories of dimethylglycine intermediates in DMGO.

(A) Representation of initial positionings of lactone intermediate in DMGO used in short molecular dynamics simulations shown in Figure 6. I, II, III, and IV indicates the spatial positioning along the trajectory as depicted in Fig 6A. Similar initial positions were used for short molecular dynamics simulations with other intermediates shown in Supp. Fig 7. (B) Comparison of single molecular dynamics trajectory of the uncharged lactone form (grey trace, as depicted in figure 6A), iminium form (brown trace), and charged lactone form (black trace) diffusion in DMGO cavity.

Supp. Fig. 6. Short MD simulations of dimethylglycine intermediates in various zones of DMGO cavity.

0.5 ns MD simulations were performed using iminium (A), charged lactone (B), and carbinolamine intermediate (C). Initial positionings of intermediates in DMGO cavity were similar as shown in Supp. Fig. 6A and are labeled as I, II, III or IV, according to Fig. 6A and Supp. Fig. 6A.

Supp. Fig. 7. Representative BD trajectories of intermediates during channeling in DMGO cavity.

Individual BD trajectories of iminium (A) and lactone (B) intermediates illustrate the absence of a common path followed by the intermediates. The trajectories were recorded during BD simulations shown in Fig. 5, and were chosen regarding their average duration of 5-6 ns. Each trajectory was sampled every 25-30 ps and is represented by lines colored according to a time scale. The volume of the cavity explored by the intermediate during the complete trajectory (i.e. unsampled) is shown as a grey could of dots. FAD and THF cofactors are rendered as Van der Waals spheres colored in cyan and pink respectively.

Supp. Fig. 8. Enzyme activity of DMGO in various mutant strains and the corresponding uncalibrated GFP-fluorescence (+/- glycine).

(A) Enzyme activities of DMGO as measured in the cell extracts of various *wt* and mutant strains and (B) the uncalibrated GFP-fluorescence measured in those strains upon exposure to dimethylglycine +/- glycine. The ratio of the fluorescence to the corresponding enzyme activity was used to calculate activity calibrated fluorescence values.

Supplement. Fig 1.

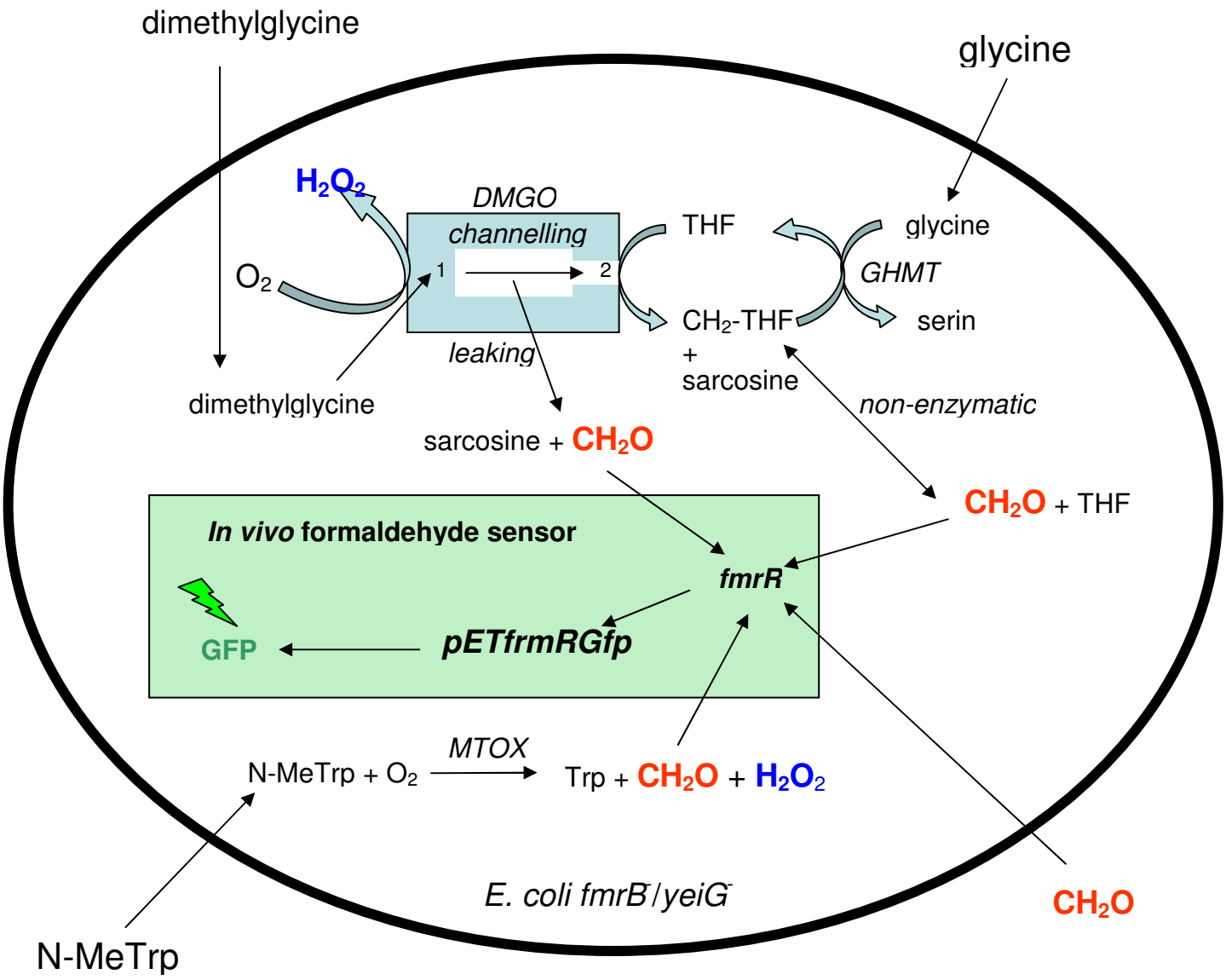

Supplement. Fig 2.

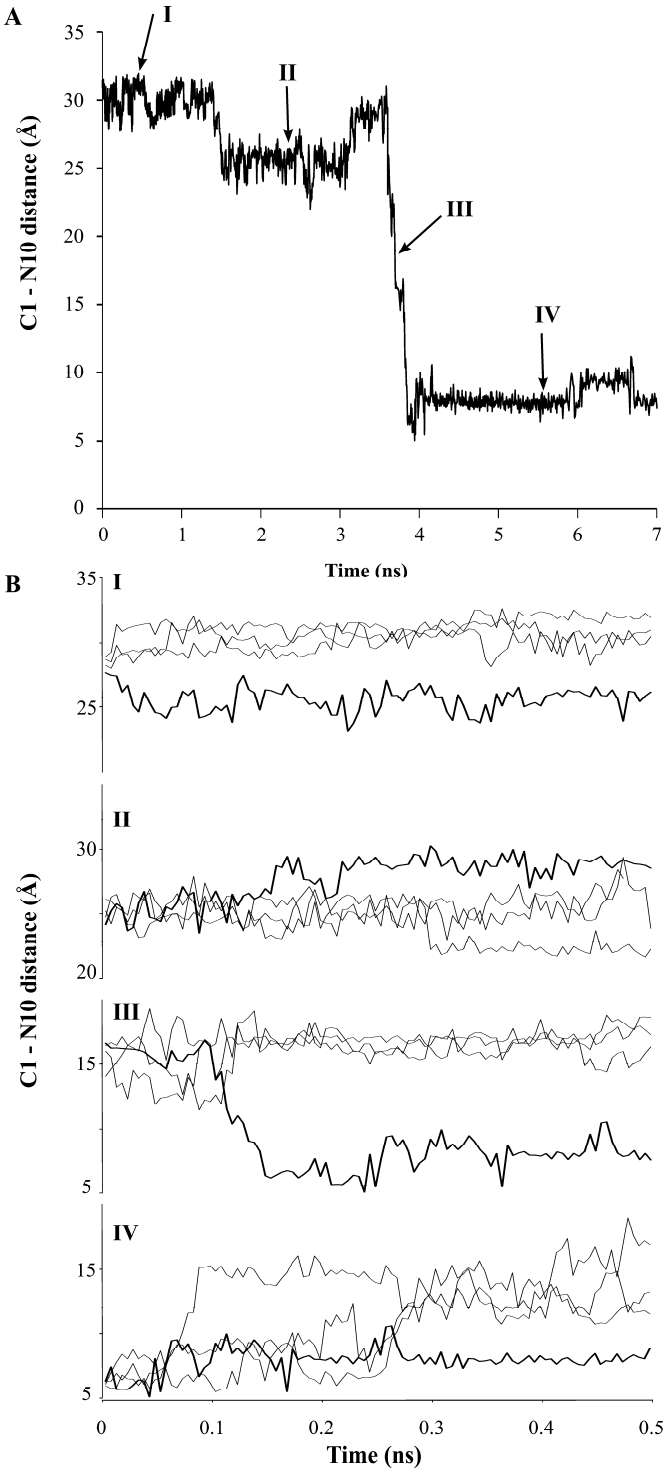

Supplement. Fig 3.

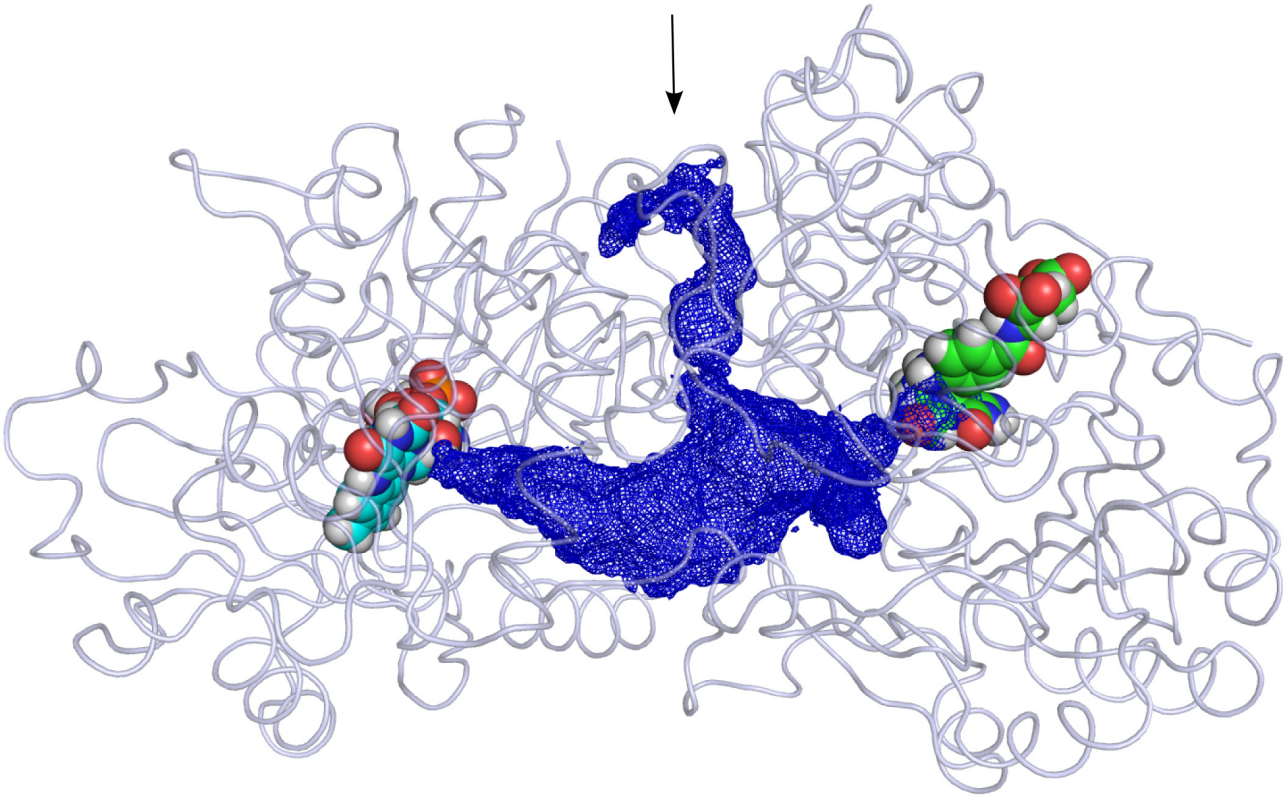

Supplement. Fig 4

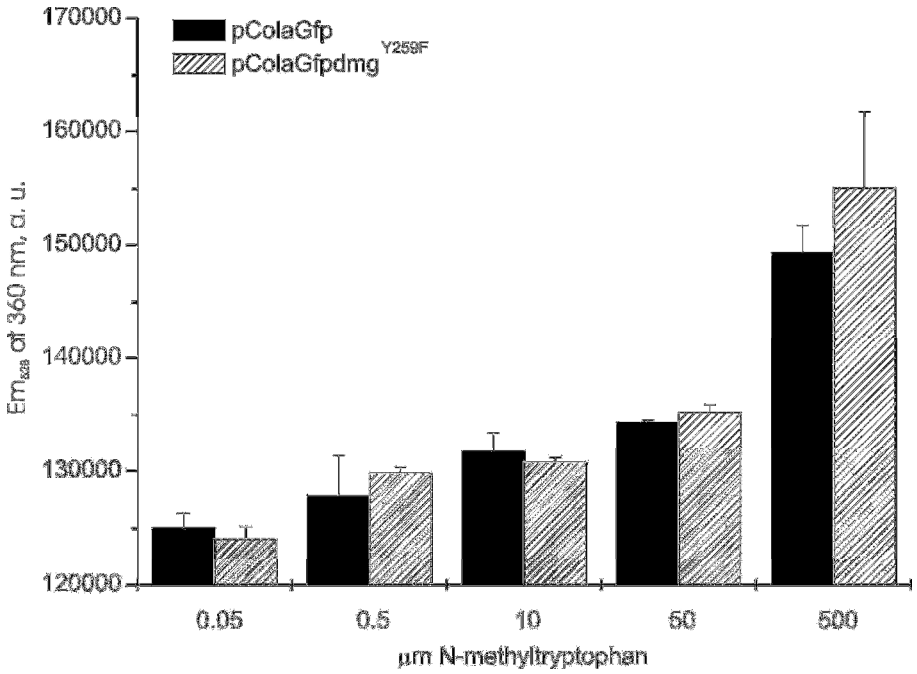

Supplement. Fig 5.

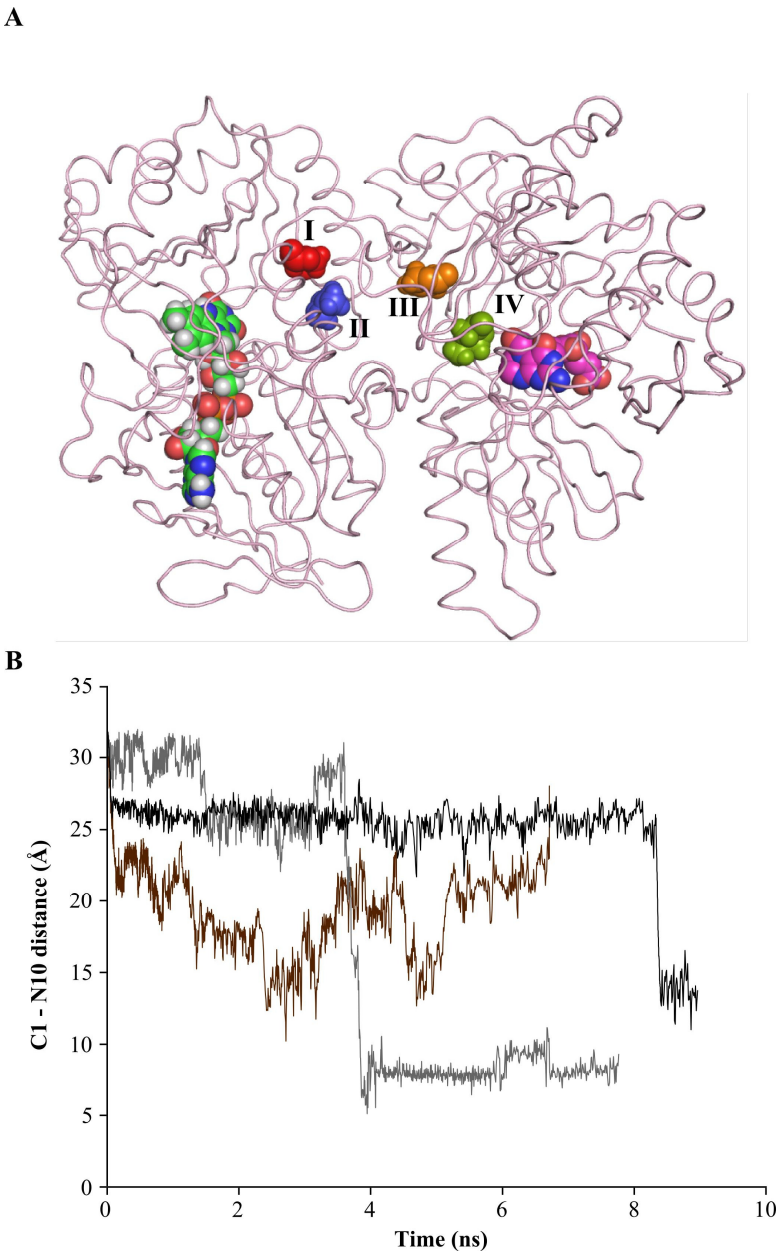

Supplement. Fig 6.

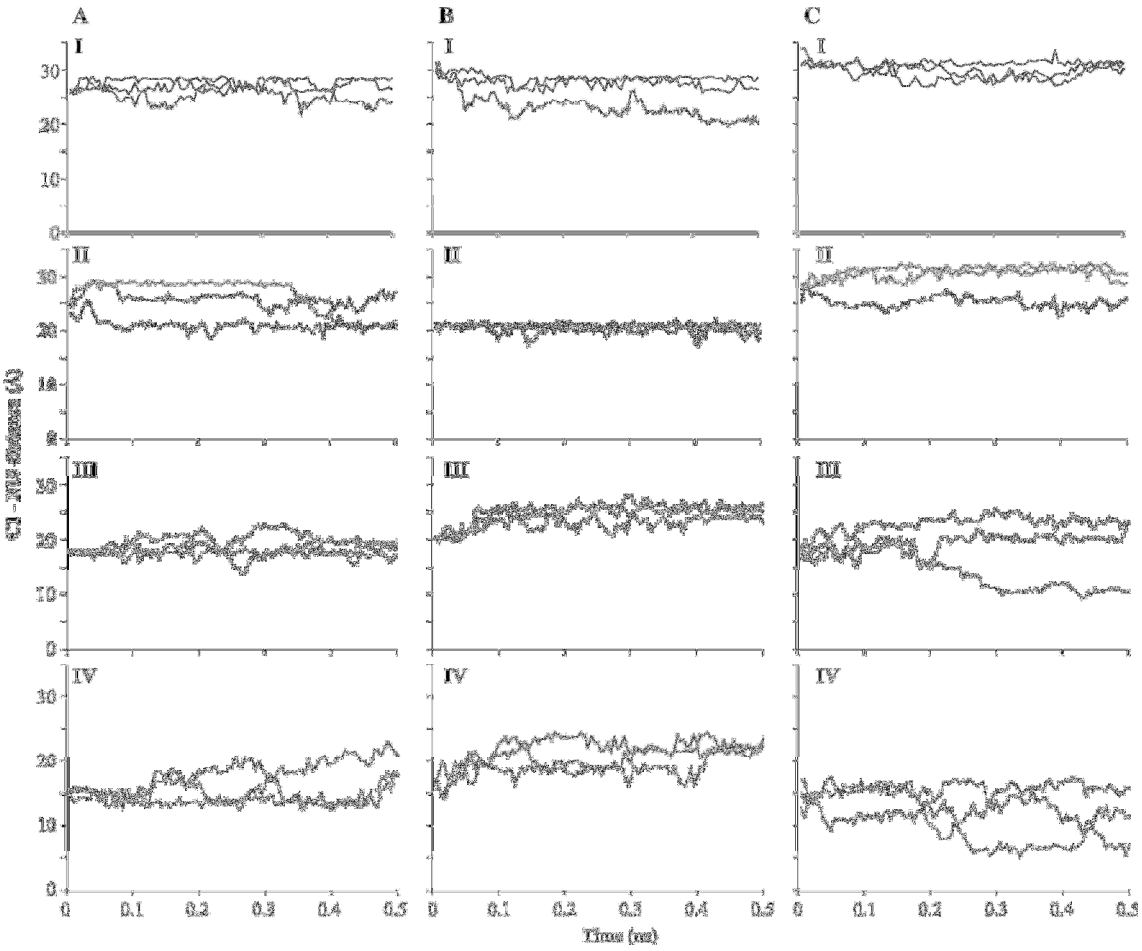

Supplement. Fig 7.

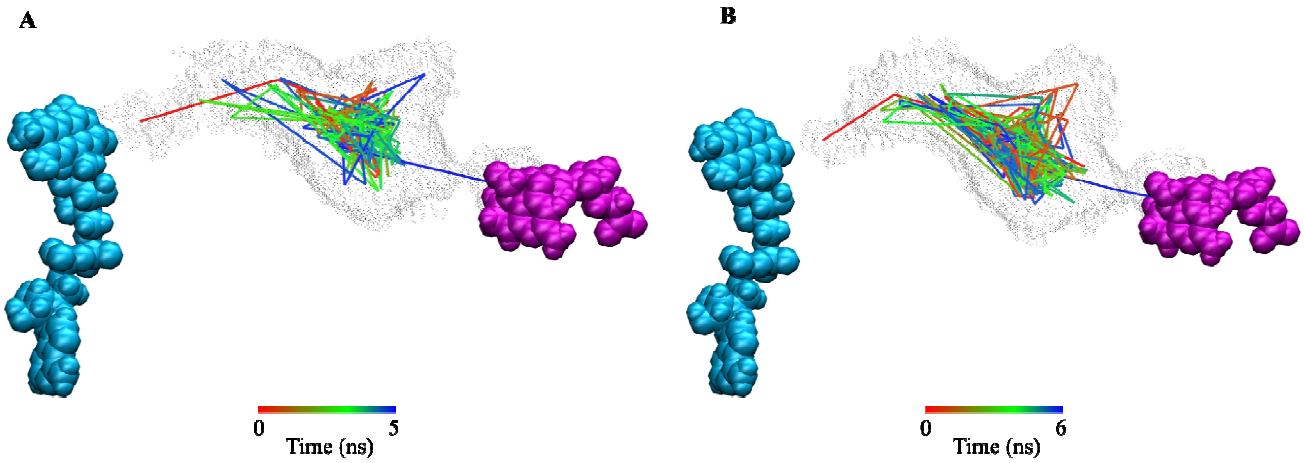

Supplement. Fig 8.